Advanced Energy Conversion Materials
http://ojs.wiserpub.com/index.php/AECM/

UNIVERSAL WISER PUBLISHER

Research Article

Non-Linear Control of Fuel Cell/Ultra-Capacitor Hybrid Electric Vehicle Using Comprehensive Function Algorithm Based on IDA-PBC

Majid Reza Naseh*, Ali Behdani

Department of Electrical Engineering, Birjand Branch, Islamic Azad University, Birjand, Iran
Email: naseh@iaubir.ac.ir.

Received: 18 September 2022; **Revised:** 4 February 2023; **Accepted:** 6 February 2023

Abstract: Hybrid electric vehicles (HEVs) have become increasingly popular due to their high fuel economy performance and low greenhouse gas emissions. HEVs that use fuel cells produce fewer emissions and are more efficient than many other types of cars. Accordingly, many researchers are significantly interested in applying a combination of the fuel cell (FC) and the ultra-capacitor (UC) for HEVs. This study proposes a method for improving the control of an FC/UC hybrid electric vehicle, also analyzing its performance. In the HEV used, the fuel cell provides the main power, but in transient situations where the FC cannot support the vehicle alone, the UC gives the stored energy to the system to solve the energy deficiency. In this study, the interconnection and damping assignment passivity-based control (IDA-PBC) method is applied and regulates the system performance under nonlinear operation. In addition, a comprehensive energy management strategy proposes to cover all driving cycle situations. The main control objective is to keep the system voltage within an acceptable range despite the appropriate dynamic behavior. To increase the accuracy of the results, in system structure modeling, energy losses are considered. In the case study part, a standard Japanese driving cycle (SJDC) uses, which comprises different practical conditions such as off-load, overload, uphill, and downhill. The simulation results using MATLAB/Simulink show the effectiveness of the proposed algorithm and control method.

***Keywords*:** fuel cell, ultra-capacitor, hybrid vehicle, passivity-based control, port controlled Hamiltonian, standard Japanese driving cycle

Nomenclature

Abbreviations

FC	Fuel cell
UC	Ultra-capacitor
PEMFC	Proton exchange membrane fuel cell
PCH	Port controlled Hamiltonian
IDA-PBC	Interconnection and damping assignment passivity-based controller
SDC	Standard driving cycle
SJDC	Standard Japanese driving cycle
HES	Hybrid energy system

DOI: https://doi.org/10.37256/aecm.4120231947

SOC	State of charge
ESS	Energy storage system
EMS	Energy management strategy

Symbols

v_{fc}	Fuel cell voltage [V]
i_{fc}	Fuel cell current [A]
$I_{fc\ \max}$	Fuel cell maximum current [A]
$I_{fc\ \min}$	Fuel cell minimum current [A]
L_{fc}	Fuel cell inductance [H]
R_{fc}	Fuel cell resistance [Ω]
m_i	Fuel cell coefficient
v_{uc}	Ultra-capacitor voltage [V]
i_{uc}	Ultra-capacitor current [A]
R_{uc}	Ultra-capacitor resistance [Ω]
L_{uc}	Ultra-capacitor inductance [H]
$v_{uc_{\max}}$	Maximum UC open circuit voltage [V]
$I_{uc\ \max}$	Ultra-capacitor maximum current [A]
$I_{uc\ \min}$	Ultra-capacitor minimum current [A]
μ_i	The duty cycle of regulator switches
x_i	The i_{th} state variable
$\tilde{x}_i$	The error of the i_{th} state variable
C_{bus}	Bus capacitance [F]
v_{bus}	Bus voltage [V]
H_d	Desired Hamiltonian of the system
Q_d	Desired structure matrix of the system
J_d	The desired interconnection system matrix
R_d	Desired damping matrix of the system
x_d	The desired equilibrium point of the system
x_{iref}	Reference state variables
p_{load}	Power demand of vehicle [W]
v	Speed of vehicle [km h^{-1}]
u	Control input vector
c_x	Drag coefficient
c_r	Rolling resistance coefficient
α	Road slope [°]
m	Vehicle mass [kg]
s	Vehicle front area [m^2]
ρ_{air}	Air density [kg m^{-3}]
g	Gravity acceleration [m s^{-2}]

1. Introduction

Greenhouse gas emissions, climate change, acid rains, and the excessive use of fossil fuels are concerns globally.

Scientists' estimations show that CO_2 emissions caused by transportation increase from 14% in 2000 up to 28% in 2050. Also, the total greenhouse gas emissions were estimated to reach up to 80% by 2050, although researchers considered reducing them [1]. At the 2015 Paris Convention, more than 200 countries signed an agreement helping reduce pollutants such as CO_2 without reducing food production. Besides, in this agreement, the 2-degree centigrade depletion in earth temperature is emphasized (Paris Convention, 2015, FCCC/CP/2015). The emissions caused by the transportation system have resulted in a significant amount of environmental and health-related damage. These emissions caused environmental problems such as increasing greenhouse gas levels and the overuse of fossil fuels. Due to the great importance of reducing environmental pollutants in recent years, numerous papers have presented the analysis of fuel consumption and emissions in the road transportation sector [2]. A hybrid electric vehicle with a hydrogen fuel cell could become an environmentally friendly practical solution to the mentioned problems. Nowadays, fuel cells have received significant attention because of their durability and acceptable efficiency. Hence FCs have been considered for various applications, such as the automotive industries, hybrid power plants, submarines, and iron production [3-6].

A fuel cell is an electrochemical device that converts the fuel energy (most of the time hydrogen) directly into direct current electricity. Among FC types, PEMFCs are more common in vehicular systems for some specific features: satisfactory operation at low temperatures, quick startup, appropriate efficiency, higher power density, and long life. The FCs are zero emission-producing and do not have any moving components in the system [7]. The FCs are also generally more efficient than internal combustion engines and can produce power in a wide range. Because of the practical FC limitations, using solitary PEMFC cannot supply the power demand in all situations. Load rapid variations result in unbalance pressure in the FC stack, fuel starvation, and FC lifetime reduction. Hence, using a suitable energy storage system (ESS) for FCs is essential. For such a combination, using batteries is a general solution. Although batteries demonstrate acceptable behavior incorporation with FC, the UC, as a newly introduced rival, is a better partner because of its rapid response time, long lifespan, and high power density [8]. The parallel structure is the most lucrative design and chosen due to fewer component constraints, higher efficiency, and more practiced energy management [9]. Moreover, in the event of one-source failure, the system can continue its function, and it improves the reliability of the whole system. FC is connected to the DC bus by the chopper boost and buck-boost converter used for UC to the continuous load power supply, determine the portion of FC and UC of supplying the demand, and finally keep the DC bus voltage tight.

Recently, various strategies have been used to control FC/UC hybrid vehicles. Fadil et al. have used a non-linear control method [10]. This article has fixed DC bus voltage, regulated UC current, and achieved closed-loop stability.

The IDA-PBC method and the Hamilton-Jacobi Bellman (HJB) optimization and optimally controlling the energy flow between the sources have been combined [11]. The source limitation is considered in terms of the battery state of charge. Wu and Lee reported reported another study on a sliding mode control (SMC) of a hybrid electric vehicle [12].

IDA-PBC is a technique used to regulate the behavior of nonlinear systems in Hamiltonian formalism. This method is based on the principles of energy shaping and dissipation and is a physically inspired control design method. The main objective of this method is to stabilize the dynamic system behavior by rendering its closed-loop (by shaping its energy) with the desired storage function (by a proper Lyapunov function). IDA-PBC is a method used to control and stabilize nonlinear systems modeled by the Port-controlled Hamiltonian (PCH) [13]. The passivity-based controller is one of the methods that has recently been considered for various applications, for example: to control robots, hybrid vehicles, power systems, etc. [14-15].

Amrouche et al. discussed the control of an FC/UC hybrid system for high instantaneous power dynamics applications [9]. In this study, an IDA-PBC method is applied to the coordination of converters of a fuel-cell system used in a hybrid electric vehicle. An energy management technique is suggested for FC/SC/battery Vehicles via IDA-PBC [16]. In this study, the energy management of an HEV in the presence of faults in the fuel cell (FC) level by holding a battery state of charge constraints is considered. Benmouna and Becherif passivity-based control and optimal control for energy management of fuel cell/battery hybrid system [17]. The novelty of the proposed energy management strategy for the studied hybrid system is the combination between interconnection and damping assignment-passivity-based control and the Hamiltonian Jacobi Bellman method. An optimized frequency decoupling EMS using the fuzzy control method was proposed to extend the fuel cell lifespan and improve fuel economy for fuel cell/battery/ultracapacitor hybrid electrical vehicles [18]. In the proposed method, a fuel cell, battery, and ultracapacitor are used to

supply components of required power, respectively. Deng et al. focuses on an energy management system with a priority on optimizing the energy distribution in hybrid railway vehicles to reduce the overall operational cost [19]. In this paper, the proposed energy management strategy (EMS) aims at minimizing hydrogen consumption and fuel-cell aging costs while achieving a favorable balance between battery charging and discharging. Behdani and Naseh reported a study of an FC/UC HEV by the IDA-PBC method [20]. This study represented a strategy to control HEV under a standard European driving cycle. In the mentioned references and other similar researches, a comprehensive view of diverse conditions for driving the vehicles, such as braking mode, constant velocity mode, and accelerating modes, has not been considered.

In this article, a comprehensive algorithm is suggested to improve the FC/UC operation and SOC management. In addition, to increase the result resolution in dynamic equations, the system losses are considered. A standard Japanese-driving cycle (JP-10-Mode, [21]) is used in the simulations to evaluate the effectiveness of the control strategy.

The rest of the paper is organized as follows: In section 2, the structure of the hybrid energy system (HES) is described. Section 3 puts forward the proposed control method for the HEV system. The suggested energy management strategy is presented in section 4. Case study results under SDC are described in section 5. Finally, the conclusion of the paper is presented in section 6.

2. System structure

Figure 1 demonstrates a typical hybrid vehicle system, which comprises a fuel cell, ultra-capacitor, and load. In this article, the load indicates the power required to thrust the vehicle. Also, the fuel cell supports the HEV in all practical situations. Another essential element is the ultra-capacitor, which stores surplus energy (for example, in brake seconds) to reuse it in necessary conditions. In this structure, to connect FC to the DC bus, a boost unidirectional converter is applied. Also, the UC is connected to the DC bus through a buck-boost bidirectional converter. Due to the operation of the elements, a parallel structure implements for the system.

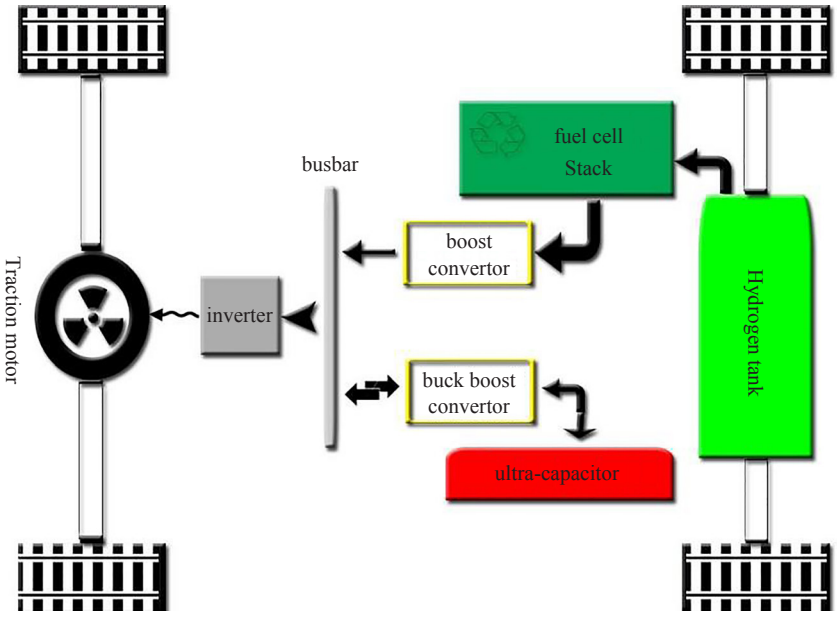

Figure 1. Fuel cell/ultra-capacitor structure

2.1 *System elements*

2.1.1 *Fuel cell*

A fuel cell is an electrochemical device that converts the energy of hydrogen (or other fuel gases like methanol) directly into electricity. Each kind of FC has a specific application due to its features. Low operation temperature, simplicity, tolerable efficiency, quick response time, and suitable power density extend PEMFC usage in automotive applications [10, 22]. Specifications of a PEMFC fuel cell is listed in Table 1 [7]. In this study, a PEMFC with the following voltage-current equation is used [23]:

$$v_{fc} = m_5 i_{fc}^5 + m_4 i_{fc}^4 + m_3 i_{fc}^3 + m_2 i_{fc}^2 + m_1 i_{fc} + m_0 \tag{1}$$

where m_i (i = 0, ..., 5) are the coefficients listed in Table 2 of the case study section.

Table 1. Specifications of a PEMFC

Type	Mobile ion	Overall chemical reaction	Efficiency (%)	Operation temperature (°C)
PEMFC	hydrogen ions	$H_2 + 1/2\,O_2 \Rightarrow H_2O$	35-60	30-100

2.1.2 *Ultra-capacitor*

Ultra-capacitor is a young preferable option because of its robustness and being maintenance-free, which separates it from other kinds of energy storage systems like batteries. UCs properties are between batteries and capacitors. UCs can instantly provide large amounts of energy, and their charging response is slower than in the case of ceramic capacitors [24]. The static charge process and a large amount of energy storage are other specifications of UCs. UCs have high power density and during transient can release energy fast enough. Hence, the use of UC is more appropriate for system transient difficulties. Moreover, charging UCs takes less time compared to batteries.

The most significant characteristic of the UCs is the state of charge (SOC), which is defined as the follows:

$$SOC = \frac{v_{uc}}{v_{uc_{\max}}} \tag{2}$$

Where $v_{uc_{\max}}$ is the maximum UC open circuit voltage and v_{uc} is the output voltage.

A bidirectional DC/DC (buck-boost) converter connects UC to the bus. In this article, to simplify the equations, a capacitor with internal resistance is considered.

2.2 *Circuit structure and dynamic model of the hybrid vehicle*

The structure of the studied hybrid electric vehicle is depicted in Figure 2. The hybrid system consists of PEMFC and UC as the sources, plus boost and buck-boost converter. The FC provides the required energy for the load as the primary power source. The UC supports the FC in fast transient situations (the conditions in that FC cannot supply the load alone).

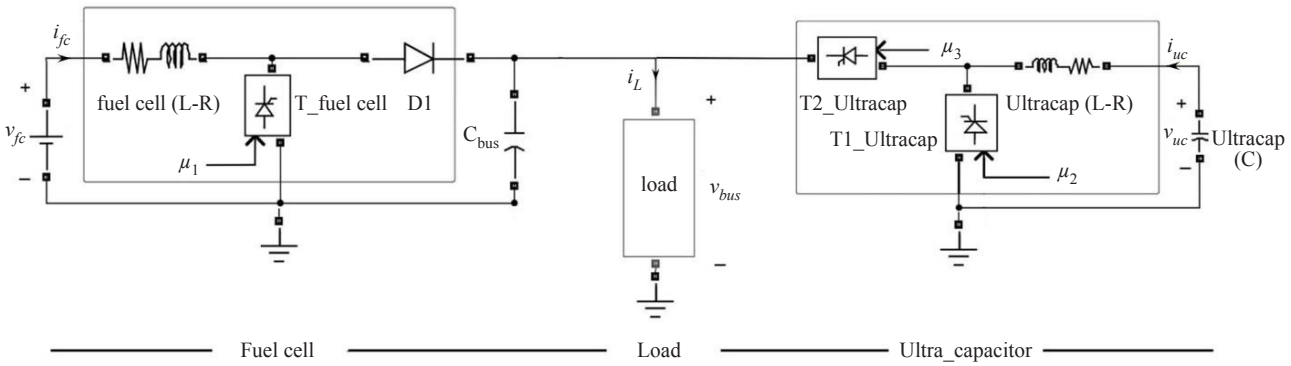

Figure 2. Structure of the studied hybrid system

According to Kirchhoff's laws, the dynamic equations of the system can be written with nonlinear equations as follows:

$$\frac{di_{fc}}{dt} = \frac{1}{L_{fc}}\left[v_{fc} - (1-\mu_1)v_{bus} - r_{fc}i_{fc}\right]$$

$$\frac{dv_{bus}}{dt} = \frac{1}{C_{bus}}\left[(1-\mu_1)i_{fc} + \mu_{23}i_{uc} - i_L\right]$$

$$\frac{di_{uc}}{dt} = \frac{1}{L_{uc}}\left[v_{uc} - \mu_{23}v_{bus} - r_{uc}i_{uc}\right] \tag{3}$$

where μ_1 and μ_{23} are the duty cycle of regulator switches and act as control inputs. μ_{23} is the control input of the buckboost converter and is defined as $1 - \mu_2$ and μ_3 in boost mode and buck mode, respectively.

By using the following variables: $x_1 = L_{fc}i_{fc}$, $x_2 = C_{bus}v_{bus}$, and $x_3 = L_{uc}i_{uc}$, the dynamic model of the system (3) can be written as follows:

$$\frac{dx_1}{dt} = -r_{fc}\frac{x_1}{L_{fc}} - (1-\mu_1)\frac{x_2}{C_{bus}} + v_{fc}$$

$$\frac{dx_2}{dt} = (1-\mu_1)\frac{x_1}{L_{fc}} + \mu_{23} - \frac{x_3}{L_{uc}} - i_L$$

$$\frac{dx_3}{dt} = v_{uc} - \mu_{23}\frac{x_2}{C_{bus}} - r_{uc}\frac{x_3}{L_{uc}} \tag{4}$$

3. Control design and analysis

In this study, the IDA-PBC approach is used to control the hybrid system. IDA-PBC is a general method that

adjusts the behavior of the nonlinear system by assigning a preferred structure to the closed-loop. This method has several advantages including the shaping of the energy besides the robustness of the control system. The central objective of the IDA-PBC methodology is to assign the state variables $x = [x_1\ x_2\ x_3]^T$ to the desired values $x_d = [x_{1ref}\ x_{2ref}\ x_{3ref}]^T$, where x_{1ref}, x_{2ref}, and x_{3ref} are the preferred values for the variables of the system (3). The idea of IDA-PBC is to find a control $u(x)$ with the purpose of rendering the system (4) in the form of port-controlled Hamiltonian (PCH) as below:

$$\dot{x} = \left(J_d - R_d\right)\nabla H_d \tag{5}$$

Where $Q_d = J_d - R_d$, and H_d are desired structure matrix, and desired Hamiltonian of the system, respectively. In addition, J_d is the interconnection matrix, and R_d is the damping matrix of the system. In order to design a controller for the mentioned system, the desired Hamiltonian function is proposed:

$$H_d(x) = \tilde{x}_1^{\,2} / 2L_{fc} + \tilde{x}_2^{\,2} / 2C_{bus} + \tilde{x}_3^{\,2} / 2L_{uc} \tag{6}$$

where $\tilde{x}_i = x_i - x_{iref}$ is the error of the i_{th} state variable.

According to IDA-PBC methodology, the desired performance is specified by dynamic as Eq. (5), where the interconnection and damping matrices are selected as:

$$J_d = \begin{bmatrix} 0 & \mu_1 - 1 & 0 \\ 1-\mu_1 & 0 & \mu_{23} \\ 0 & -\mu_{23} & 0 \end{bmatrix};\ R_d = \begin{bmatrix} r_{11} & 0 & 0 \\ 0 & r_{22} & 0 \\ 0 & 0 & r_{33} \end{bmatrix} \tag{7}$$

From equation (6), the gradient of the desired Hamiltonian of the system is:

$$\nabla H_d = \left[\tilde{x}_1 / L_{fc}\ \tilde{x}_2 / C_{bus}\ \tilde{x}_3 / L_{uc}\right]^T \tag{8}$$

Using equations (7) and (8), given of the form:

$$\left(J_d - R_d\right)\nabla H_d = \begin{bmatrix} -r_{11}\dfrac{\tilde{x}_1}{L_{fc}} + \left(\mu_1 - 1\right)\dfrac{\tilde{x}_2}{C_{bus}} \\ \dfrac{\left(1-\mu_1\right)\tilde{x}_1}{L_{fc}} - r_{22}\dfrac{\tilde{x}_2}{C_{bus}} + \mu_{23}\dfrac{\tilde{x}_3}{L_{uc}} \\ -\mu_{23}\dfrac{\tilde{x}_2}{C_{bus}} - r_{33}\dfrac{\tilde{x}_3}{L_{uc}} \end{bmatrix} \tag{9}$$

From Eq. (4) and Eq. (9), it results in the following equation:

$$\begin{cases} -r_{11}\dfrac{\tilde{x}_1}{L_{fc}}+\dfrac{(\mu_1-1)\tilde{x}_2}{C_{bus}}=-\dfrac{r_{fc}}{L_{fc}}x_1-\dfrac{x_2}{C_{bus}}+\dfrac{x_2}{C_{bus}}\mu_1+v_{fc} \\ \dfrac{(1-\mu_1)\tilde{x}_1}{L_{fc}}-\dfrac{r_{22}\tilde{x}_2}{C_{bus}}+\dfrac{\mu_{23}\tilde{x}_3}{L_{uc}}=\dfrac{x_1}{L_{fc}}-\dfrac{x_1\mu_1}{L_{fc}}+\dfrac{x_3\mu_{23}}{L_{uc}}-i_L \\ -\mu_{23}\dfrac{\tilde{x}_2}{C_{bus}}-r_{33}\dfrac{\tilde{x}_3}{L_{uc}}=-\dfrac{r_{sc}}{L_{uc}}x_3-\dfrac{x_2}{C_{bus}}\mu_{23}+v_{uc} \end{cases} \tag{10}$$

Eq. (10) leads to the matching equations as:

$$\begin{cases} \dfrac{-x_{2ref}\mu_1}{C_{bus}}+\dfrac{r_{11}x_{1ref}}{L_{fc}}+\dfrac{x_{2ref}}{C_{bus}}-\dfrac{r_{11}-r_{fc}}{L_{fc}}x_1-v_{fc}=0 \\ \dfrac{x_{1ref}\mu_1}{L_{fc}}+\dfrac{x_{3ref}\mu_{23}}{L_{uc}}-\dfrac{x_{1ref}}{L_{fc}}+\dfrac{r_{22}x_{2ref}}{C_{bus}}-\dfrac{r_{22}x_2}{C_{bus}}-i_L=0 \\ \dfrac{-x_{2ref}\mu_{23}}{C_{bus}}+\dfrac{r_{33}x_{3ref}}{L_{uc}}-\dfrac{r_{33}-r_{uc}}{L_{uc}}x_3-v_{sc}=0 \end{cases} \tag{11}$$

Therefore, the equations of the system can be explained as:

$$\begin{cases} \dfrac{-r_{11}\tilde{x}_1}{L_{fc}}-\dfrac{x_{2ref}(\mu_1-1)}{C_{bus}}+\dfrac{r_{fc}x_1}{L_{fc}}-v_{fc}=0 \\ \dfrac{-r_{22}\tilde{x}_2}{C_{bus}}+\dfrac{x_{1ref}(\mu_1-1)}{L_{fc}}+\dfrac{x_{3ref}\mu_{23}}{L_{uc}}-i_L=0 \\ \dfrac{-r_{33}\tilde{x}_3}{L_{uc}}-\dfrac{x_{2ref}\mu_{23}}{C_{bus}}+\dfrac{r_{sc}x_3}{L_{uc}}-v_{uc}=0 \end{cases} \tag{12}$$

One of the solutions for Eq. (12), r_{22} is equal to zero, $r_{11} = r_{fc}$, and $r_{33} = r_{sc}$. The control law in boost mode and buck mode is:

I. Boost mode:

$$\mu_1=1-\frac{C_{bus}\left(v_{fc}L_{fc}+r_{11}\tilde{x}_1-r_{fc}x_1\right)}{x_{2ref}L_{fc}} \tag{13}$$

$$\mu_2=1-\frac{C_{bus}\left(v_{uc}L_{uc}+r_{33}\tilde{x}_3-r_{uc}x_3\right)}{x_{2ref}L_{uc}} \tag{14}$$

II. Buck mode:

$$\mu_3=\frac{C_{bus}\left(v_{uc}L_{uc}+r_{33}\tilde{x}_3-r_{uc}x_3\right)}{x_{2ref}L_{uc}} \tag{15}$$

In order to support the system stability, the Hamiltonian function H_d must have an isolated minimum at the desired equilibrium point x_d, furthermore conditions $J_d = -J_d^T$ and $R_d = R_d^T \geq 0$ must be satisfied, which are maintained steady in all situations of vehicle work conditions.

In general form, the power balance is satisfied by the following relations:

Consumption mode:

a. Fuel cell supply the load solitary:

$$i_{fcref} = \frac{v_{fc} - \sqrt{v_{fc}^2 - 4v_{bus}r_{fc}i_L}}{2r_{fc}} \tag{16}$$

b. Fuel cell and ultra-capacitor supply the load in collaboration:

$$i_{fcref} = i_{fc\max}$$

$$i_{ucref} = \frac{v_{uc} - \sqrt{v_{uc}^2 - 4r_{uc}\left(v_{bus}i_L - v_{fc}i_{fc\max} + r_{fc}i_{fc\max}^2\right)}}{2r_{uc}} \tag{17}$$

Braking mode:

The kinetic energy of the vehicle absorbed by the ultracapacitor:

$$i_{ucref} = \frac{v_{uc} - \sqrt{v_{uc}^2 - 4v_{bus}r_{uc}i_L}}{2r_{uc}} \tag{18}$$

4. Energy management strategy

Energy management in vehicles includes energy-related factors, such as managing energy loss, minimizing fuel consumption, etc. This paper has focused on improving the FC/UC operation and SOC management. In Figure 3, the proposed energy management strategy (EMS) flowchart is presented. This part focuses on different modes that a vehicle should work on it. These modes are represented with seven statements as below:

I. The FC can supply the load power ($0 < I_L < I_{fc\ \max}$), and UCs *SOC* is under $SOC_{o\_\min}$: FC works with its maximum power, and excess generated power of FC reserve in UC. (For the proper performance of a hybrid vehicle in normal working conditions, it is better to specify an optimal upper and lower limit for charging. These values are called $SOC_{o\_\max}$ and $SOC_{o\_\min}$. These limits guarantee that the ultracapacitor can store excess energy or produce the required power in the normal working conditions of the car.)

II. The FC can supply the load power ($0 < I_L < I_{fc\ \max}$), and UCs *SOC* is over $SOC_{o\_\max}$: FC is off, and reserved energy in UC supports the load.

III. The FC can supply the load power ($0 < I_L < I_{fc\ \max}$), and UCs *SOC* is between $SOC_{o\_\min}$ and $SOC_{o\_\max}$: UC is off, and FC in according with the load power is on.

IV. Vehicle is in braking mode, and the UC has not fully charged ($I_L < 0$ and $SOC < SOC_{\max}$): in this case, the traction motor switches into generating mode and charges the UC.

V. Vehicle brakes, but the UC has fully charged ($I_L < 0$ and $SOC > SOC_{\max}$): a mechanical brake stops the vehicle, and both power sources should be off ($SOC_{\max}$ refers to the maximum amount of charge of the ultracapacitor without damaging it).

VI. Vehicle is uphill, and the UC can support the system because it is charged ($I_L > I_{fc\ max}$ and $SOC > SOC_{min}$): the load needs power more than FCs capacity, consequently the load support by sources together.

VII. Vehicle is uphill, but the UC cannot help the system because of its low charge ($I_L > I_{fc\ max}$ and $SOC < SOC_{min}$): FC cannot provide the load power alone, therefore, it works with maximum power, and the UC stays off. Moreover, the driver should reduce speed, or use additional sources (like gasoline) instead (SOC_{min} refers to the minimum amount of charge of the ultracapacitor without damaging it).

The following values are used in the case study section:

$SOC_{max} = 90\%$, $SOC_{min} = 10\%$, $SOC_{o\_max} = 50\%$, $SOC_{o\_min} = 40\%$.

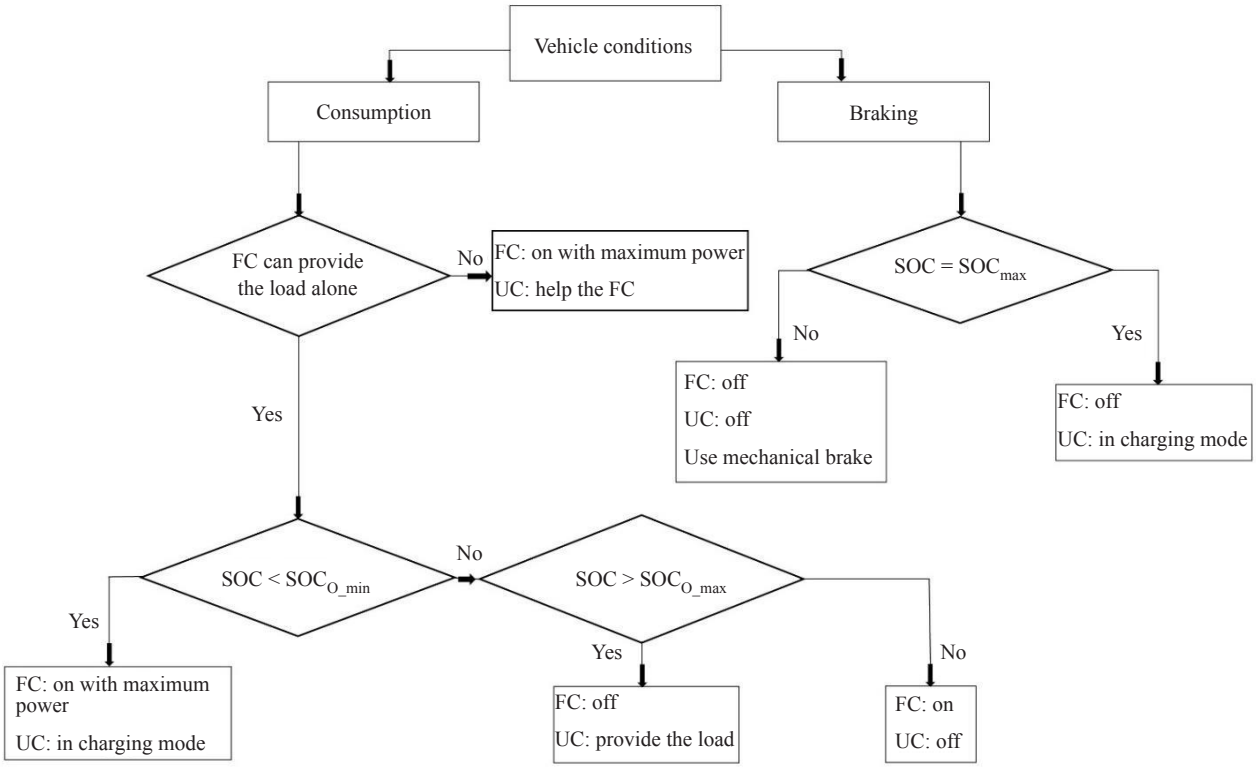

Figure 3. Energy management strategy flowchart

5. Case study results

In this section, to evaluate the suggested control method and energy management strategy, the simulation results are presented (MATLAB/Simulink software version 2017 is used). In Table 2, the system parameters for Fuel cell, Ultra-capacitor, and automotive vehicle are listed. In this part, the hybrid vehicle performance under practical conditions with the proposed control method is investigated. All possible modes for the automotive vehicle have been explored, and different situations are considered, such as general working and braking circumstances. Next, to verify the system performance, the Japanese standard driving cycle (JP-10-Mode) was employed for the suggested method [21]. According to variations of the vehicle velocity, power demand calculates by Eq. (19):

$$p_{load} = 0.5\rho_{air} v^3 s c_x + mv\left(\frac{dv}{dt} + g\sin\alpha + g c_r \cos\alpha\right) \tag{19}$$

Where v is the velocity, other characteristics of the vehicle are also given in Table 2 [20].

Table 2. System parameters

Ultracapacitor	Fuel cell	Automotive vehicle
	$R_{fc} = 20 \times 10^{-3}$ [Ω]	
	$L_{fc} = 300 \times 10^{-6}$ [H]	
	$I_{fc\ max} = 30$ [A]	$\rho_{air} = 1.225$
$C_{uc} = 12$ [F]	$I_{fc\ min} = 0$ [A]	$c_x = 0.3$
$R_{uc} = 10 \times 10^{-3}$ [Ω]	$m_0 = 60$	$c_r = 0.01$
$L_{uc} = 100 \times 10^{-6}$ [H]	$m_1 = -1.17$	$m = 400$ [kg]
$I_{uc\ max} = 70$ [A]	$m_2 = 0.0617$	$\alpha = 0$ [°]
$I_{uc\ min} = 0$ [A]	$m_3 = -0.0016$	$s = 1.4$ [m^2]
	$m_4 = 1.98 \times 10^{-5}$	$g = 9.8$ [m s^{-2}]
	$m_5 = -9.01 \times 10^{-8}$	

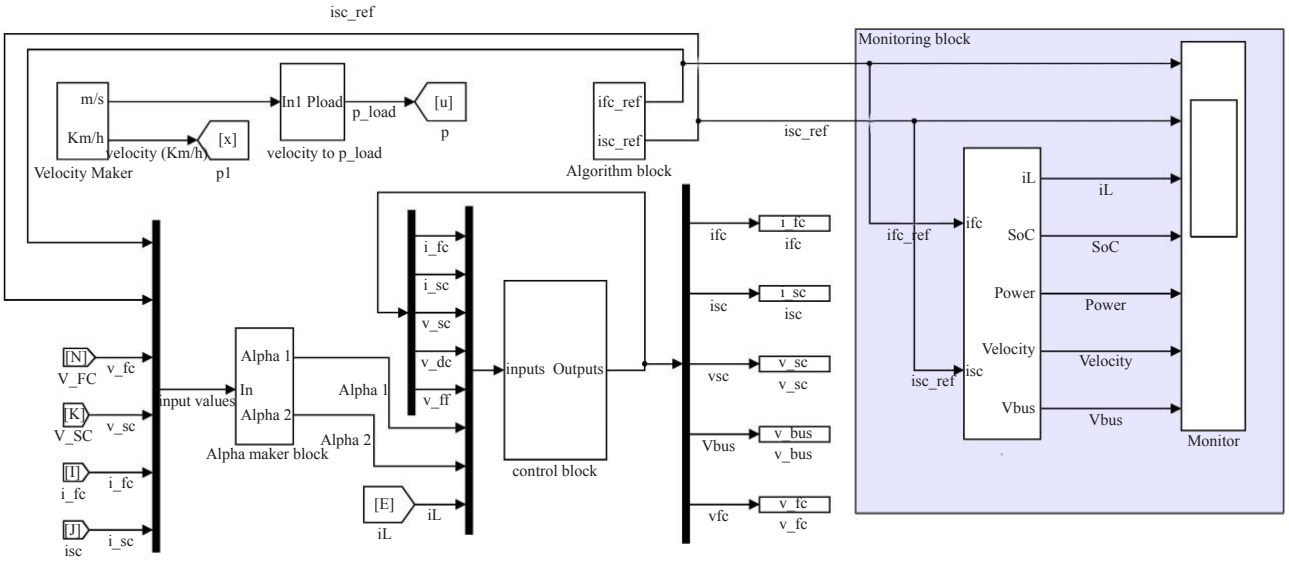

Figure 4. The simulated system

The system-simulated circuit is given in Figure 4, and consists of the following parts:

1. Velocity and p_{load} block: this part produces the demand power of load according to the standard velocity curve.

2. Fire angle maker: in this segment, μ_1 and μ_2, μ_3 as the duty cycles of the chopper boost and buck-boost converter are represented.

3. Algorithm block: different driving modes of the vehicle are considered in this part.

4. Monitoring block: in this section, velocity and other parameters are demonstrated on an oscilloscope.

5. Control block: system equations and control strategy is implemented in this segment.

For the simulation part, it is better to choose a driving cycle that includes most of the situations that may arise in

practice while driving. One of the suitable choices is the Japanese driving cycle. In Figure 5a, the employed standard Japanese driving cycle (JP-10-Mode) is given. In this study, a critical velocity curve is selected among standard driving cycles, aiming to challenge the controlling method and represented algorithm. According to Eq. (19), power alternations of the automotive vehicle are achieved from SDC and illustrated in Figure 5b. The figures also illustrate fluctuations in braking moments and it takes places after 80 s when the velocity increases up to about 40 km/h. Equations (16-18) are used to calculate the reference currents for FC and UC, these currents produce the best ideal results. Figure 5c shows the fuel cell voltage-current specification.

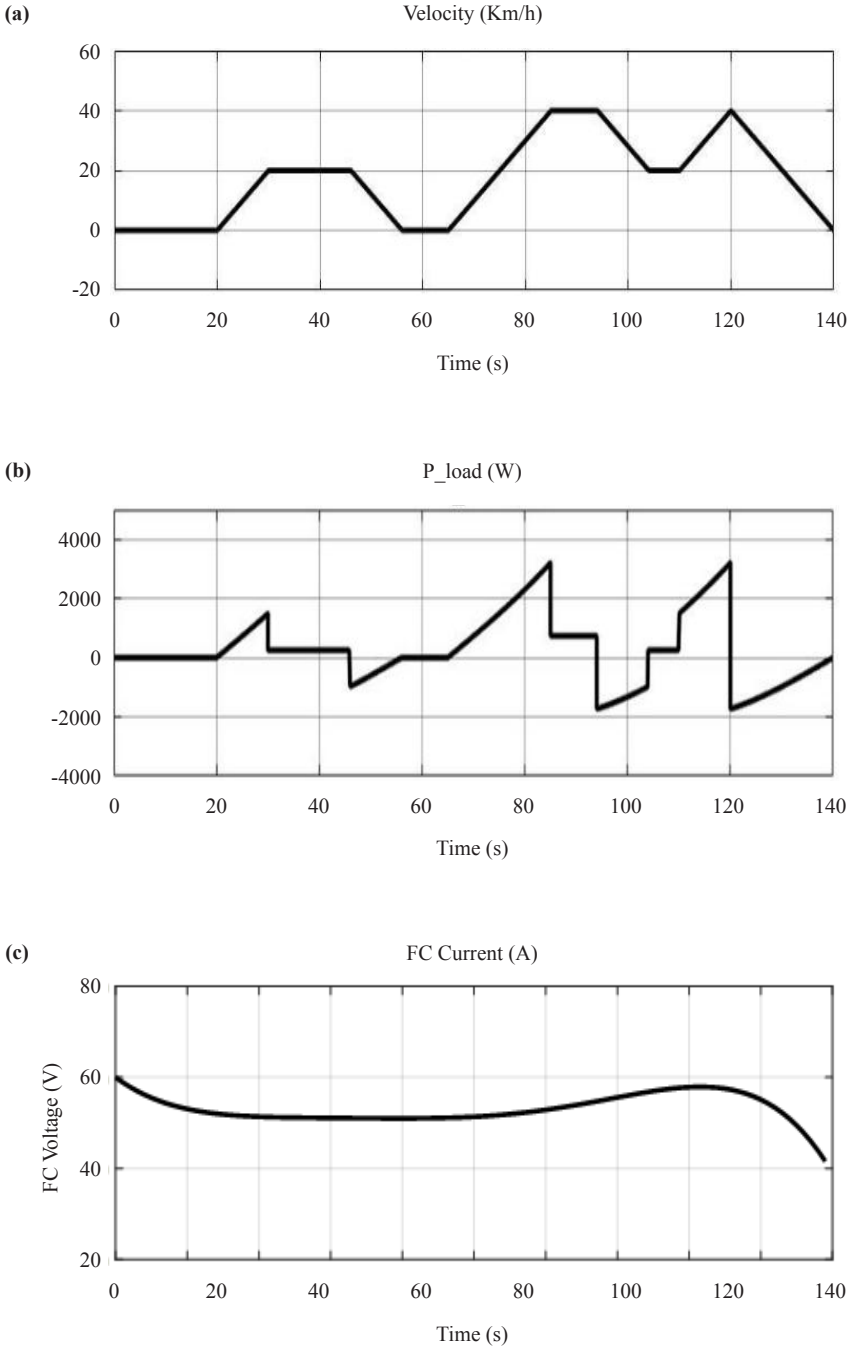

Figure 5. a. JP-10-MODE standard velocity driving cycle; b. Power demand of the vehicle according to SDC; c. Fuel cell voltage-current specification.

Figures 6 and 7 represent the actual voltages and currents of FC and UC respectively. Simulations show that actual circuit currents can follow reference currents well. UC voltage variation is smooth as depicted using such ESS instead of others guaranteeing the whole system's appropriate operation.

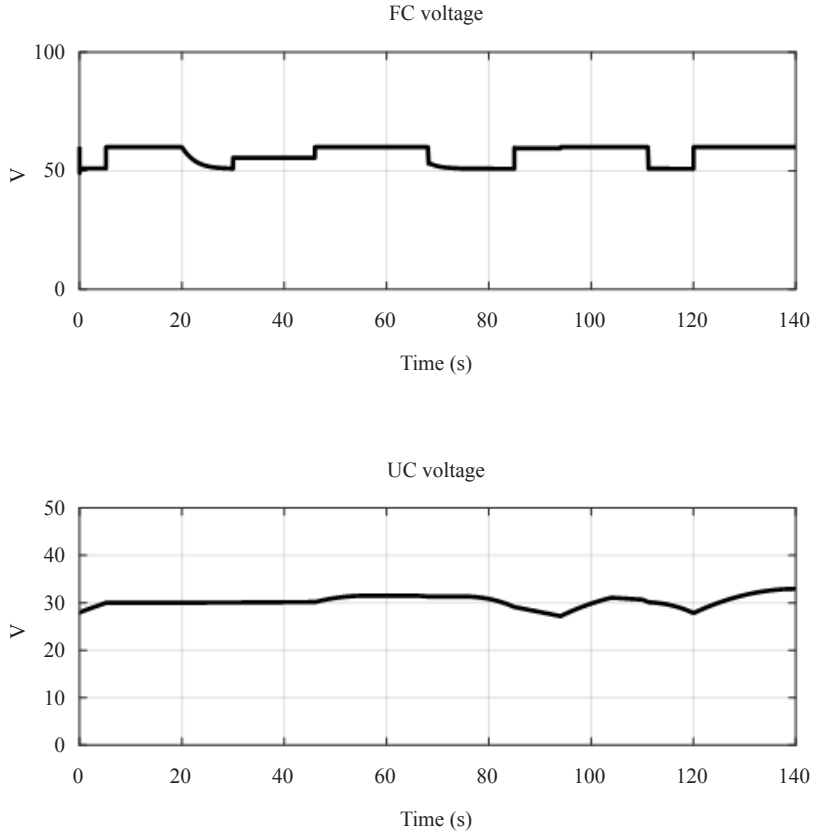

Figure 6. FC and UC voltages

The overall bus voltage of the system and a critical moment zoom is given in Figure 8. As it is shown, v_{bus} alters from 50 V up to near 80 V. In this article, a challenging SDC is selected. The selected driving cycle has remarkably difficult control moments, however, the results show that the DC bus voltage remains at an acceptable level.

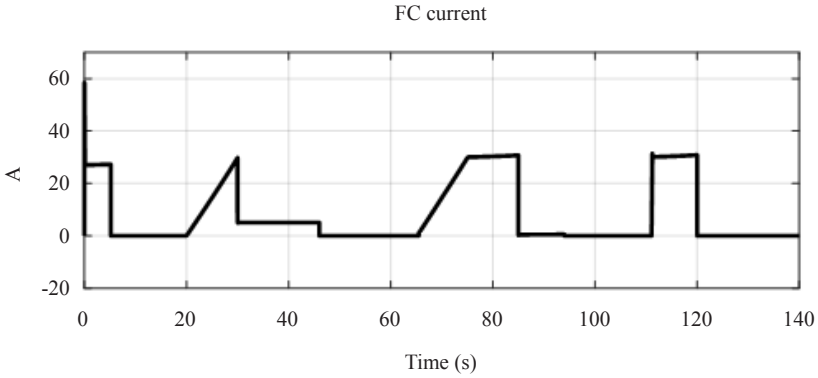

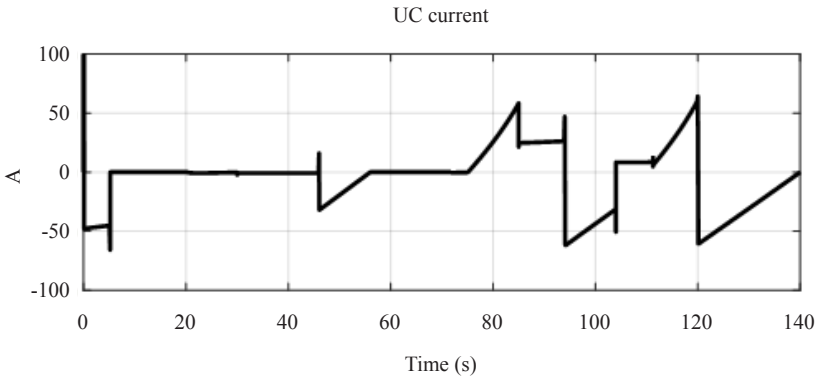

Figure 7. FC and UC currents

Figure 8 represents the state of charge alternations. In (0-5 s) and (80-85 s), the SOC is out of range and not stable. In practical situations, to improve the reliability of the system, it needs to establish SOC within a specific range (50%-60%).

The proposed control strategy tries to return the SOC to the acceptable range as soon as possible. In Figure 9, zoom-in time illustrates that critical alternations of the v_{bus} damped rapidly (under 0.02 s).

In the following, we will check the performance of the car in different periods:

0-20sec:

In the beginning, the charge of UC is less than $SOC_{o\_\max}$, so FC turns on and charges UC up to $SOC_{o\_\max}$ (about 5 seconds). After that, because the speed is zero, UC and FC are turned off.

20-30sec:

The car is accelerating and operates in mode III of the proposed EMS in section 4 (FC: On, UC: Off).

30-45sec:

The car moves at a constant speed and operates in mode III of the proposed EMS (FC: On, UC: Off).

45-55sec:

Braking (Reduce speed): The vehicle operates in mode IV of the proposed EMS (FC: Off, UC: Charging).

55-65sec:

Vehicle speed is zero, so UC and FC are off.

65-75sec:

The car is accelerating and operates in mode III (FC: On, UC: Off).

75-85sec:

The car is accelerating and operates in mode VI (FC: MAX, UC: On).

85-95sec:

The car moves at a constant speed and operates in mode II (FC: Off, UC: On).

95-105sec:

Braking (Reduce speed): The vehicle operates in mode IV (FC: Off, UC: Charging).

105-110sec:

The car moves at a constant speed and operates in mode II (FC: Off, UC: On).

110-120sec:

The car is accelerating and operates in mode VI (FC: MAX, UC: On).

120-140sec:

The car is decelerating the speed and operates in mode IV (FC: Off, UC: Charging).

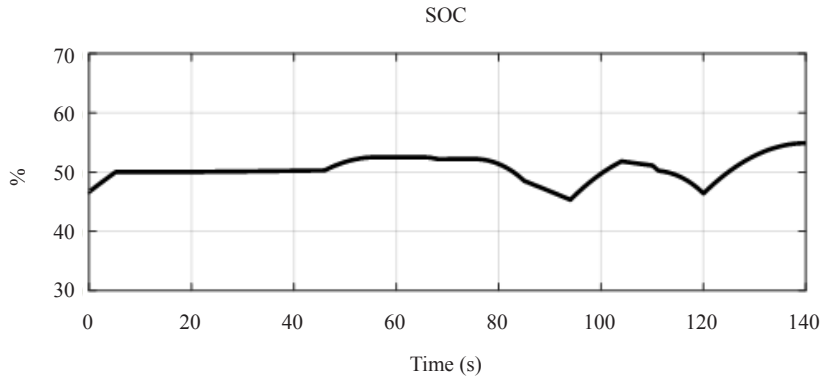

Figure 8. SOC of the UC

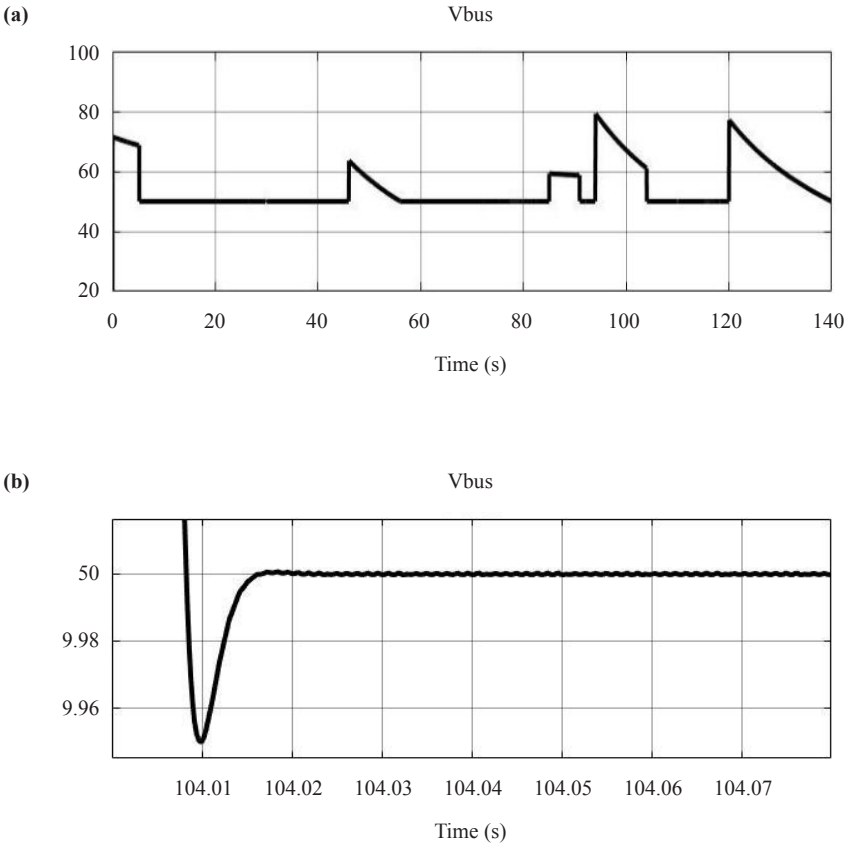

Figure 9. a. the DC bus voltage, b. Zoom on the critical seconds

6. Conclusion

This paper has presented an energy management strategy and a method to control a hybrid electric vehicle. The HEV consists of a typical fuel-cell/ultra-capacitor operating in practical situations. The suggested energy management strategy attempts to keep SOC in an acceptable range. The interconnection and damping assignment passivity-based control (IDA-PBC) method is used to energy-shaping and adjusts the DC bus voltage, in all practical circumstances for an HEV. The simulations show one of the advantages of the proposed control method, which minimizes fluctuations in

control signals and reduces the depreciation of the system components. In this study to analyze the HEV performance, standard-Japanese-driving-cycle JP-10-Mode was employed, and acceptable system behavior in all circumstances was approved. The controlling method has several advantages, such as short response time despite fast load alternation, fewer calculations that help reduce computation time, and high stability against load variations. The simulation results confirm the effectiveness of the control method under different practical conditions, such as off-load, overload, uphill, and downhill.

Conflict of interest

The authors declare that there is no conflict of interest regarding the publication of this paper.

References

[1] Ambrose AF, Al-Amin AQ, Rasiah R, Saidur R, Amin N. Prospects for introducing hydrogen fuel cell vehicles in Malaysia. *International Journal of Hydrogen Energy.* 2017; 42(14): 9125-9134. Available from: https://doi.org/10.1016/j.ijhydene.2016.05.122.

[2] Al-Osaimi S, Sreekanth K, Al-Foraih R, Al-Kandari S. Trends in road transportation fuel consumption and carbon emissions: A scenario analysis using system dynamic modelling. *International Journal of Sustainable Energy.* 2020; 39(4): 349-361. Available from: https://doi.org/10.1080/14786451.2019.1696343.

[3] Bizon N. Efficient fuel economy strategies for the fuel cell hybrid power systems under variable renewable/load power profile. *Applied Energy.* 2019; 251: 113400. Available from: https://doi.org/10.1016/j.apenergy.2019.113400.

[4] Corral-Vega PJ, García-Triviño P, Fernández-Ramírez LM. Design, modelling, control and techno-economic evaluation of a fuel cell/supercapacitors powered container crane. *Energy*. 2019; 186: 115863. Available from: https://doi.org/10.1016/j.energy.2019.115863.

[5] Olabi AG, Wilberforce T, Abdelkareem MA. Fuel cell application in the automotive industry and future perspective. *Energy*. 2021; 214: 118955. Available from: https://doi.org/10.1016/j.energy.2020.118955.

[6] Luo Y, Wu Y, Li B, Mo T, Li Y, Feng S-P, et al. Development and application of fuel cells in the automobile industry. *Journal of Energy Storage.* 2021; 42: 103124. Available from: https://doi.org/10.1016/j.est.2021.103124.

[7] Nehrir MH, Wang C. 6-Fuel cells. In: Rashid MH. (eds.) *Electric Renewable Energy Systems*. Boston: Academic Press; 2016. p.92-113.

[8] Li T, Liu H, Zhao D, Wang L. Design and analysis of a fuel cell supercapacitor hybrid construction vehicle. *International Journal of Hydrogen Energy.* 2016; 41(28): 12307-12319.

[9] Amrouche B, Cherif TO, Ghanes M, Iffouzar K. A passivity-based controller for coordination of converters in a fuel cell system used in hybrid electric vehicle propelled by two seven phase induction motor. *International Journal of Hydrogen Energy.* 2017; 42(42): 26362-26376. Available from: https://doi.org/10.1016/j.ijhydene.2017.08.099.

[10] Fadil HE, Giri F, Guerrero JM, Tahri A. Modeling and nonlinear control of a fuel cell/supercapacitor hybrid energy storage system for electric vehicles. *IEEE Transactions on Vehicular Technology.* 2014; 63(7): 3011-3018. Available from: https://doi.org/10.1109/TVT.2014.2323181.

[11] Benmouna A, Becherif M, Depernet D, Dépature C, Boulon L. Nonlinear control and optimization of hybrid electrical vehicle under sources limitation constraints. *International Journal of Hydrogen Energy,* 2019; 45(19): 11255-11266. Available from: https://doi.org/10.1016/j.ijhydene.2018.12.227.

[12] Wu G, Lee KY. Sliding mode control of a hybrid fuel cell-battery power system. *IFAC-PapersOnLine*. 2015; 48(30): 512-517. Available from: https://doi.org/10.1016/j.ifacol.2015.12.431.

[13] Ortega R, Schaft AVD, Maschke B, Escobar G. Interconnection and damping assignment passivity-based control of port-controlled Hamiltonian systems. *Automatica.* 2002; 38(4): 585-596. Available from: https://doi.org/10.1016/S0005-1098(01)00278-3.

[14] Benmouna A, Becherif M, Dépature C, Boulon L, Depernet D. Experimental study of energy management of FC/SC hybrid system using the Passivity Based Control. *International Journal of Hydrogen Energy.* 2018; 43(25): 11583-11592.

[15] Back J, Ha W. Robust tracking of robot manipulators via momentum-based disturbance observer and passivity-based controller. *International Journal of Control, Automation and Systems.* 2019; 17(4): 976-985.

[16] Benmouna A, Becherif M, Depernet D, Ebrahim MA. Novel energy management technique for hybrid electric

vehicle via interconnection and damping assignment passivity based control. *Renewable Energy.* 2018; 119: 116-128. Available from: https://doi.org/10.1016/j.renene.2017.11.051.
[17] Benmouna A, Becherif M. Combined passivity based control and optimal control for energy management of fuel cell/battery hybrid system. *Asian Journal of Control.* 2019; 21(4): 1857-1868.
[18] Fu Z, Zhu L, Tao F, Si P, Sun L. Optimization based energy management strategy for fuel cell/battery/ultracapacitor hybrid vehicle considering fuel economy and fuel cell lifespan. *International Journal of Hydrogen Energy.* 2020; 45(15): 8875-8886. Available from: https://doi.org/10.1016/j.ijhydene.2020.01.017.
[19] Deng K, Liu Y, Hai D, Peng H, Löwenstein L, Pischinger S, et al. Deep reinforcement learning based energy management strategy of fuel cell hybrid railway vehicles considering fuel cell aging. *Energy Conversion and Management.* 2022; 251: 115030. Available from: https://doi.org/10.1016/j.enconman.2021.115030.
[20] Behdani A, Naseh MR. Power management and nonlinear control of a fuel cell-supercapacitor hybrid automotive vehicle with working condition algorithm. *International Journal of Hydrogen Energy.* 2017; 42(38): 24347-24357. Available from: https://doi.org/10.1016/j.ijhydene.2017.07.197.
[21] Barlow TJ, Latham S, McCrae I, Boulter P. *A reference book of driving cycles for use in the measurement of road vehicle emissions*. TRL Published Project Report, TRL; 2009.
[22] Aouzellag H, Ghedamsi K, Aouzellag D. Energy management and fault tolerant control strategies for fuel cell/ultra-capacitor hybrid electric vehicles to enhance autonomy, efficiency and life time of the fuel cell system. *International Journal of Hydrogen Energy*. 2015; 40(22): 7204-7213.
[23] Aiteur IE, Vlad C, Godoy E. Energy management and control of a fuel cell/supercapacitor multi-source system for electric vehicles. *2015 19th International Conference on System Theory, Control and Computing (ICSTCC)*. Cheile Gradistei, Romania; 2015. Available from: https://doi.org/10.1109/ICSTCC.2015.7321392.
[24] Libich J, Máca J, Vondrák J, Čech O, Sedlaříková M. Supercapacitors: Properties and applications. *Journal of Energy Storage.* 2018; 17: 224-227.